Advanced Zemax Simulations of Optical Transition/Diffraction Radiation

A. Aryshev[1], T. Aumeyr[2], M. Billing[3], L. Bobb[2,4], B. Bolzon[4,5,6], E. Bravin[4], P. Karataev[2], K. Kruchinin[2], T. Lefevre[4], S. Mazzoni[4], M. Shevelev[1], N. Terunuma[1], J. Urakawa[1]

1. KEK, Ibaraki, Japan
2. John Adams Institute at Royal Holloway, Egham, Surrey, UK
3. Cornell University, Ithaca, New York, USA
4. CERN European Organisation for Nuclear Research, Geneva, Switzerland
5. Cockcroft Institute, Worrington, Cheshire, UK
6. University of Liverpool, Liverpool, Merseyside, UK

Contents

- Introduction & Motivation
- What is Zemax?
- Theory
- OTR simulations
- ODR simulations
- Conclusions

Introduction

- Next generation LC (CLIC, ILC) and also X-Ray FELs require transverse beam size measurements with µm resolution:
  - Wire scanner: disturbs the beam; can be destroyed by high intensity beams.
  - Laser-wire: non-invasive high resolution measurements; many are required over long distances (cost, maintenance)
- OTR: charged particle crosses a boundary between two media with different dielectric properties
  - Widely used for transverse profile measurements
  - OTR monitors: simple, robust and give direct image of 2D beam profile
  - OTR PSF structure: extract beam size with sub-µm resolution
  - Invasive method: degrade beam properties or beam can destroy target → diagnose low intensity pilot beams
- ODR: charged particle moves in the vicinity of a medium.
  - Spatial-spectral properties are sensitive to various beam parameters.
  - Energy loss due very small, beam parameters are unchanged → non-invasive diagnostics

Zemax

Zemax 13 Release 2

- Readily available commercial optical design software: standard tool to conceptualise, design, optimise, analyse and tolerance optical systems.
- Geometrical ray tracing is incomplete description of light propagation.
- Coherent process: wavefront travels through free space and interferes with itself → physical optics.
- Physical Optics Propagation (POP): Zemax mode that calculates wavefront propagation through an optical system surface by surface.
- Target as radiation source: initial electric field defined in 2D matrix (binary or text) or computed with Windows Dynamic Link Library (DLL).
- In POP: wavefront modelled with this array (dimension, sampling and aspect ratio are user-definable).
- Array then propagated in free space between optical surfaces → transfer function is computed at each surface → matrix is propagated from one side to the other.
- In this way, simulation of any source of light is possible (e.g. TR, DR, synchrotron radiation (SR)).

Electric source field

Y-polarisation component electric field for the induced by a single electron on a target surface [1]:

$$\Re\{E_y\} = \frac{2e}{\gamma\lambda\cos\theta_0}\left\{\frac{y}{\rho}K_1\left[\frac{2\pi}{\beta\gamma\lambda}\rho\right]\cos\phi\cos\theta_0 + \frac{1}{\gamma}K_0\left[\frac{2\pi}{\beta\gamma\lambda}\rho\right]\sin\phi\sin\theta_0\right\}$$

$$\Im\{E_y\} = \frac{2e}{\gamma\lambda\cos\theta_0}\left\{\frac{y}{\rho}K_1\left[\frac{2\pi}{\beta\gamma\lambda}\rho\right]\sin\phi\cos\theta_0 - \frac{1}{\gamma}K_0\left[\frac{2\pi}{\beta\gamma\lambda}\rho\right]\cos\phi\sin\theta_0\right\}$$

$$\text{with } \beta = \sqrt{1-\tfrac{1}{\gamma^2}},\ \text{phase shift } \phi = ky\tan\theta_0\left(1-\tfrac{1}{\beta}\right),\ k = \tfrac{2\pi}{\lambda} \text{ and } \rho = \sqrt{x^2+y^2}.$$

x and *y* are two orthogonal coordinates of the target measured from the point of electron incidence, *γ* is the charged particle Lorentz factor, *λ* is the radiation wavelength, θ_0 is the angle between the trajectory of the particle and the screen plane, K_0 and K_1 are the zeroth and first order modified Bessel function. For TR the entire field is reflected and propagates towards the observation plane.

[1] D. V. Karlovets and A. P. Potylitsyn, Nucl. Instrum. Meth. B266, 3738 (2008).

OTR

Angular distribution of intensity in the far-field of a charged particle passing through a boundary between vacuum and an ideal conductor with ultra-relativistic approximation (θ_x, θ_y, $\gamma^{-1} \ll 1$) [2]

[2] A. P. Potylitsyn, Nucl. Instrum. Meth. B145, 169 (1998).

$$\frac{d^2W_y^{TR}}{d\omega d\Omega} = \frac{\alpha}{\pi^2} \frac{{\theta_y}^2}{\left(\gamma^{-2} + {\theta_x}^2 + {\theta_y}^2\right)^2} \frac{1}{\left(1 - \theta_y \cot\theta_0\right)^2}$$

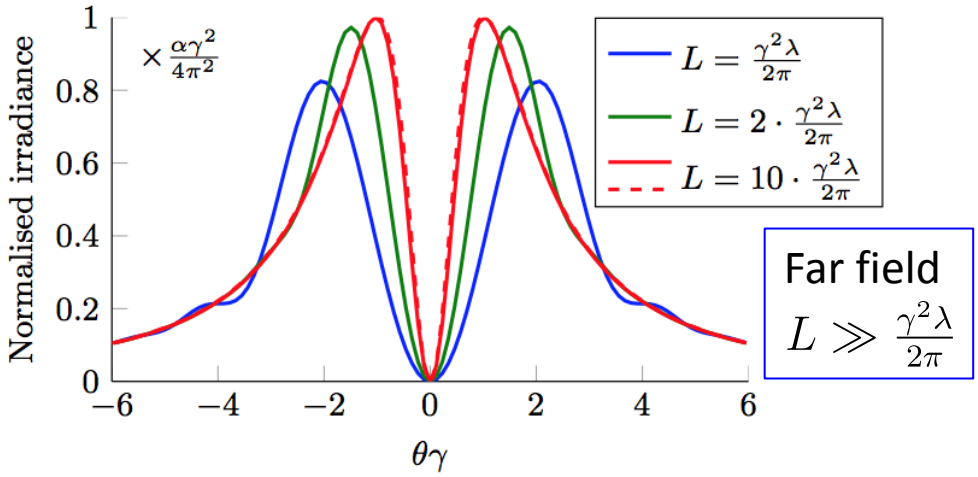

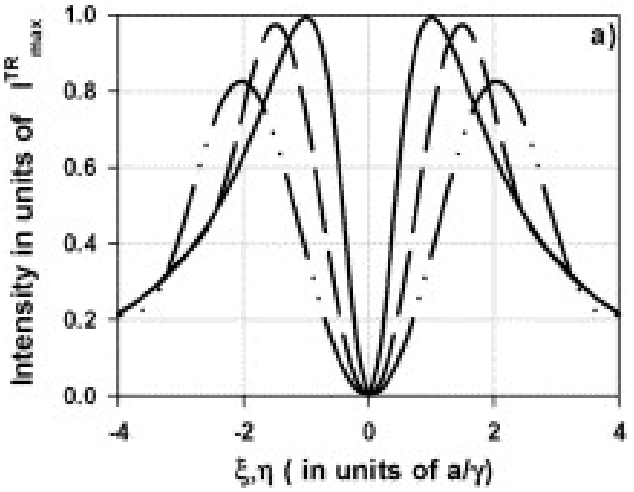

FIG. 1. Comparison between theoretical (dashed) and simulated (solid) TR angular distribution for various distances between source and image plane L ($\lambda = 550$ nm, $\gamma = 2500$, $\theta_x = 0$).

[3] P. V. Karataev, Phys. Lett. A 345, 428 (2005).

OTR PSF

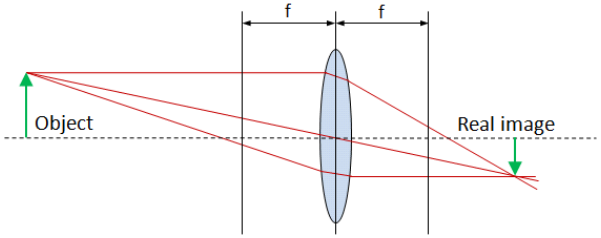

Resolution of OTR monitors is normally defined as a root-mean-square of the so-called point spread function (PSF). The OTR PSF has a structure itself which can be used to extract the beam size with sub-µm resolution resolution.

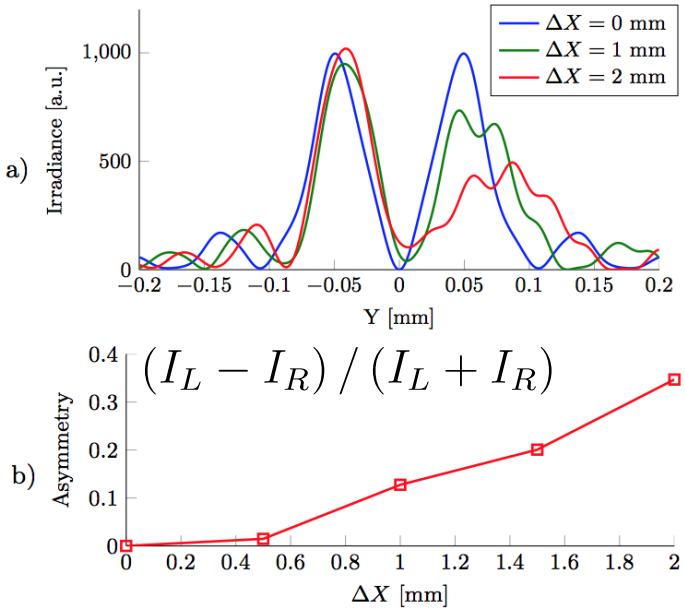

FIG. 4. TR PSF (a) and asymmetry (b) for various horizontal lens offsets ΔX ($\lambda = 550$ nm, $\gamma = 2500$, $\theta_x = 0$, $M = -7.4$).

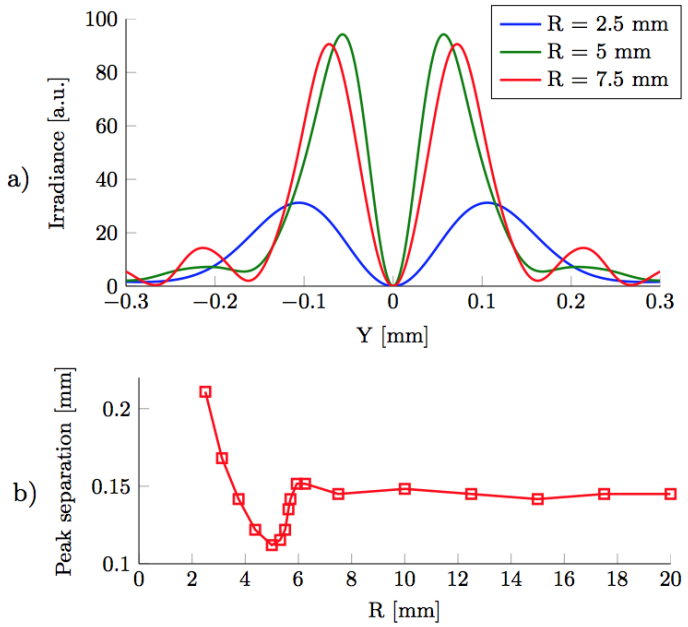

FIG. 6. TR PSF (a) and distance between the two main lobes (b) for various lens radii R ($\lambda = 550$ nm, $\gamma = 2500$, $\theta_x = 0$, $M = -10$).

Diffraction causes the peaks to move closer together until the effect dominates and the peaks move apart again.

ODR – circular aperture

Charged particle moving normally through the centre of a circular hole in an infinitely thin, perfectly conducting disc [4]

[4] A. P. Potylitsyn et al., Springer Tracts Mod. Phys. 239, 1 (2011).

$$E_y(\mathbf{r},\omega) = \frac{ie}{\pi\gamma}\frac{F(b)-F(a)}{\gamma^{-2}+{\theta_x}^2+{\theta_y}^2} \qquad F(a) = ak\theta J_0(ak\theta)K_1\left(\frac{a\omega}{v\gamma}\right) + \frac{a\omega}{v\gamma}J_1(ak\theta)K_0\left(\frac{a\omega}{v\gamma}\right)$$

$$\frac{d^2W_y^{hole}}{d\omega d\Omega} = 4\pi^2|E_y|^2$$

incident field radius

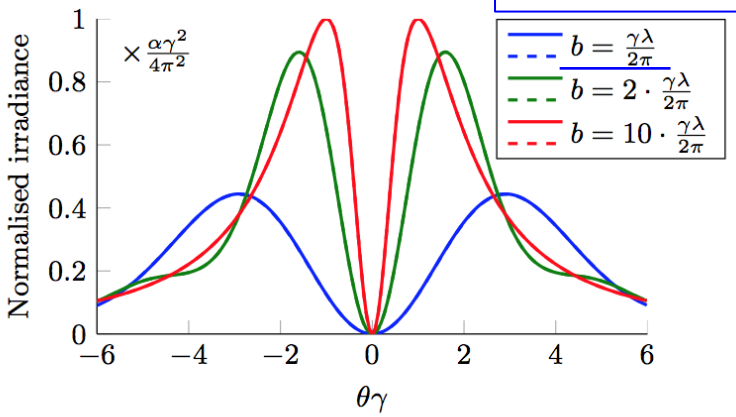

FIG. 7. Comparison between theoretical (dashed) and simulated (solid) DR angular distribution in the far-field for various target disc radii b ($\lambda = 400$ nm, $\gamma = 4110$, $\theta_x = 0$, $a = 1$ nm).

infinitely small hole

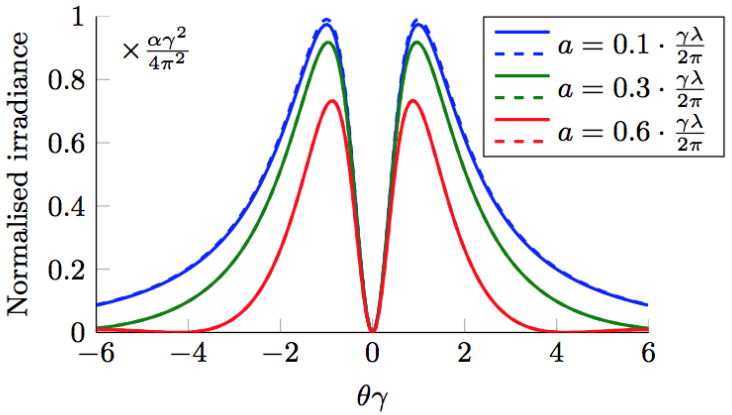

FIG. 8. Comparison between theoretical (dashed) and simulated (solid) DR angular distribution in the far-field for various hole radii a ($\lambda = 400$ nm, $\gamma = 4110$, $\theta_x = 0$, $b = 10\frac{\gamma\lambda}{2\pi}$).

infinite target

ODR – circular aperture – beam offset

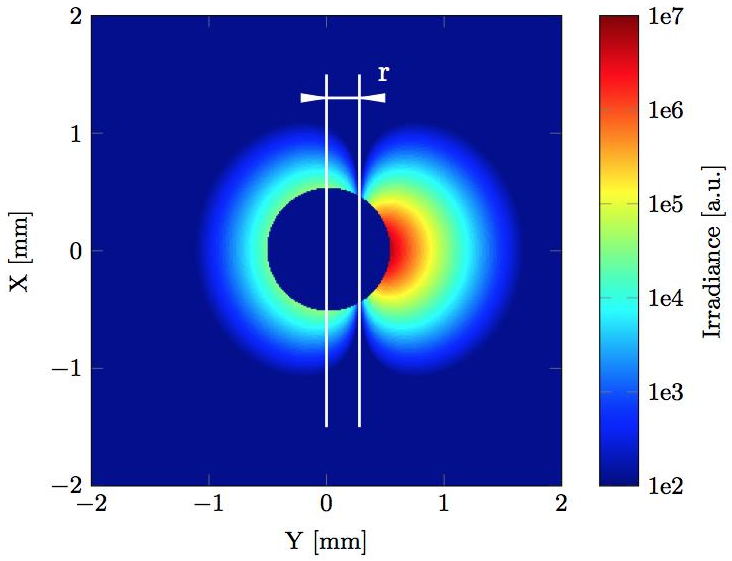

FIG. 10. Electric field at the source for single electron passing through circular hole with a beam offset of $r = \frac{\gamma\lambda}{2\pi}$ ($\lambda = 400$ nm, $\gamma = 4110$, $a = 2\frac{\gamma\lambda}{2\pi}$).

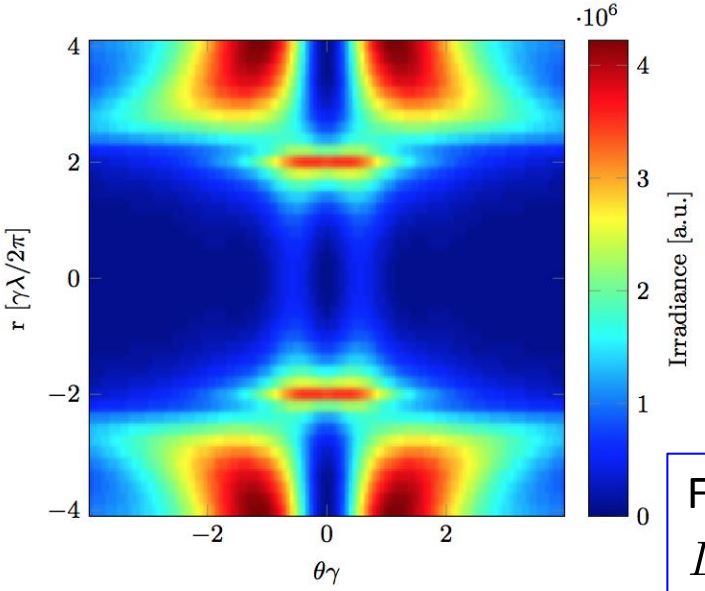

FIG. 11. DR angular distribution in the far-field for various beam offsets r ($\lambda = 400$ nm, $\gamma = 4110$, $a = 2\frac{\gamma\lambda}{2\pi}$, $L = 100\frac{\gamma^2\lambda}{2\pi}$).

Far field

$$L \gg \frac{\gamma^2\lambda}{2\pi}$$

Each horizontal line represents the cross-section of the angular distribution for a beam of a certain offset. Starting with a beam offset of $r = -4\gamma\lambda/2\pi$, the distribution is almost pure TR. The closer the beam moves to the centre of the hole, the more DR like the distribution becomes. When moving the beam up even more, TR is established again for a beam offset of $r = 4\gamma\lambda/2\pi$.

ODR – circular aperture – beam offset

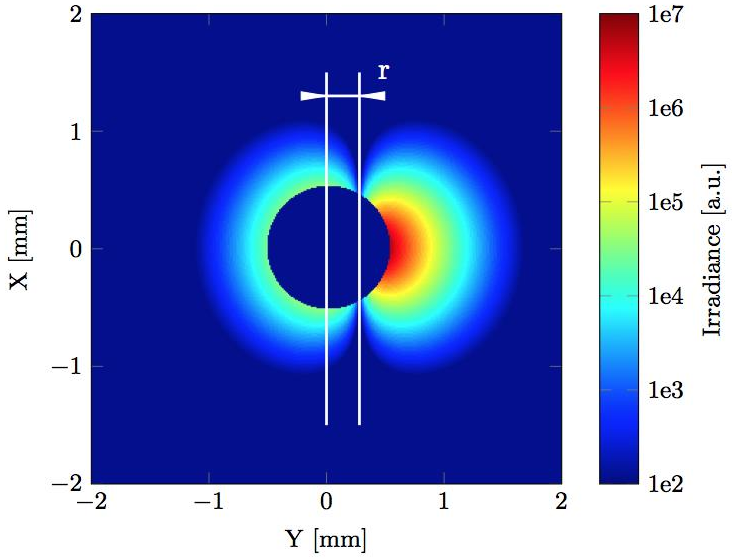

FIG. 10. Electric field at the source for single electron passing through circular hole with a beam offset of $r = \frac{\gamma\lambda}{2\pi}$ ($\lambda = 400$ nm, $\gamma = 4110$, $a = 2\frac{\gamma\lambda}{2\pi}$).

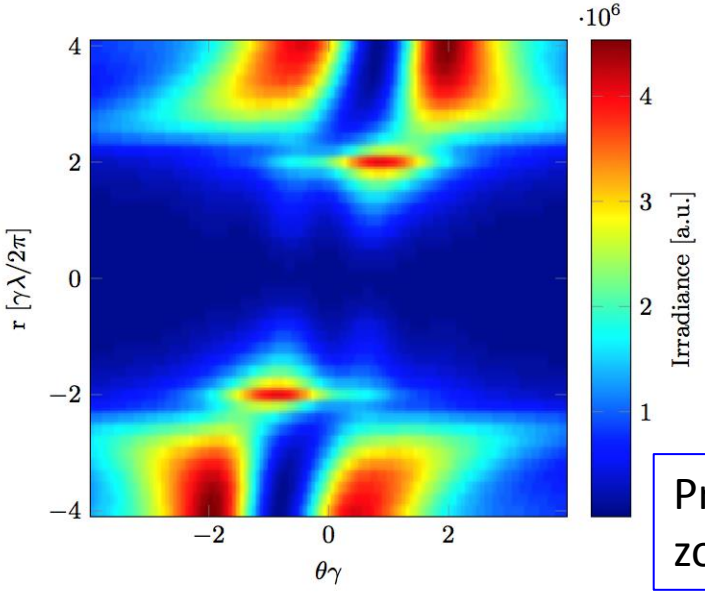

FIG. 12. DR angular distribution in the pre-wave zone for various beam offsets r ($\lambda = 400$ nm, $\gamma = 4110$, $a = 2\frac{\gamma\lambda}{2\pi}$, $L = 5\frac{\gamma^2\lambda}{2\pi}$).

Pre-wave zone

In the pre-wave zone an asymmetry can be found. This originates from the interference of the radiation from different parts of the target.

ODR – arbitrary aperture

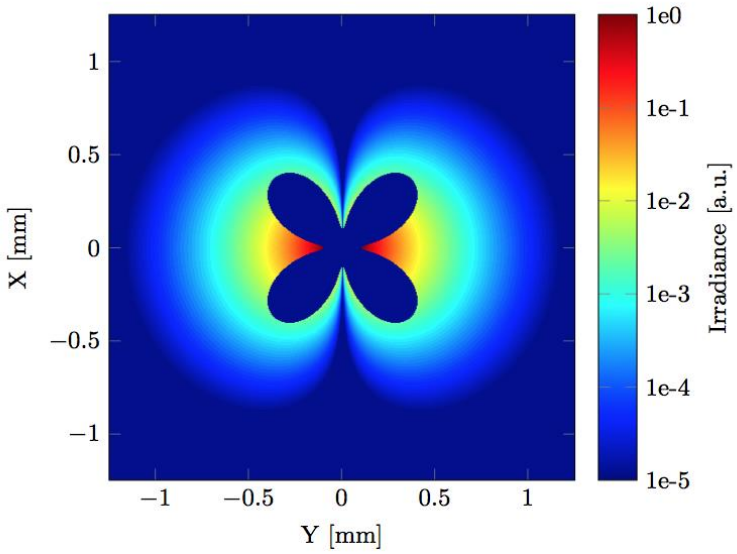

FIG. 17. Vertically polarised electric field at the source for a four-leafed aperture ($\lambda = 400$ nm, $\gamma = 4110$, $a = 2\frac{\gamma\lambda}{2\pi}$).

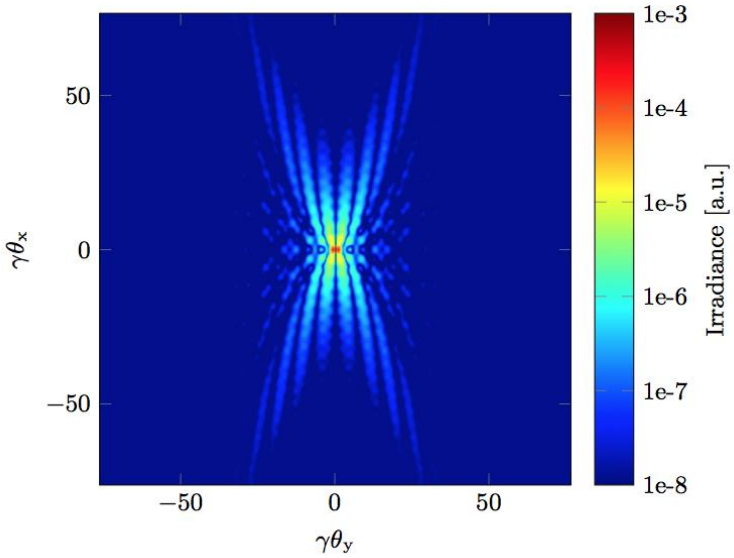

FIG. 18. DR angular distribution vertical polarisation for a four-leafed aperture in the far-field ($\lambda = 400$ nm, $\gamma = 4110$, $a = 2\frac{\gamma\lambda}{2\pi}$, $L = 10\frac{\gamma^2\lambda}{2\pi}$).

Conclusions

- With assumptions similar to theoretical boundary conditions, Zemax simulations of TR and DR agree with the analytical expressions.
- Off-axis incident field or an arbitrarily shaped aperture does not slow down the Zemax simulations noticeably and is therefore the preferable method.
- Finite beam size: displacing the single particle with respect to the optical axis across the transversal profile → angular pattern for each step can then be weighted and summed up.
- This tool represents the most comprehensive approach to the design of a real diagnostics based on either OTR or ODR including all misalignment errors (shifts, tilts) and optimisation of a real optical system (including viewports, polarisers, filters, etc.).

Thank you for your attention!

Any questions?